Inorganic Chemistry
Communication

Inorg. Chem. **2010**, *49*, 8647–8649 **8647**
DOI: 10.1021/ic100558x

Novel Functionalized Metal−Organic Framework Based on Unique Hexagonal Prismatic Clusters

Qi Yue,[†] Li Yan,[†] Jian-Yong Zhang,[†] and En-Qing Gao*[,†,‡]

[†]*Shanghai Key Laboratory of Green Chemistry and Chemical Processes, Department of Chemistry, East China Normal University, Shanghai 200062, China, and* [‡]*State Key Laboratory of Structure Chemistry, Fujian Institute of Research on the Structure of Matter, Chinese Academy of Sciences, Fuzhou 350002, China*

Received March 25, 2010

The novel porous 3D metal−organic framework synthesized from fluorenone-2,7-dicarboxylate contains zinc−glycolate−carboxylate layers in which the unique hexagonal prismatic $[Zn_6(OCH_2CH_2O)_6]$ clusters are connected by planar $[Zn_3(OCH_2CH_2O)(COO)_2]$ motifs; the pore surface is furnished with carbonyl groups and open metal sites.

Recently, much attention has been paid to porous metal−organic frameworks (MOFs) owing to the scientific interest in the creation of nanometer-sized spaces and their high prospects for practical applications.[1−3] The development of MOFs has benefited much from the great tendency of metal ions to generate some recurrent polynuclear motifs with specific ligands. Many robust MOFs with di-, tri-, and tetranuclear or higher-nuclear metal carboxylate clusters as secondary building units (SBUs) have been constructed.[4] The discovery and identification of new polynuclear motifs bearing special structural features is always important because they may bring in new properties/functions in MOFs.[5] On the other hand, the pore-surface properties are essentially important for adsorption and catalysis applications, and hence modification of the pore surface is currently being pursued in the field of MOFs. Although MOFs with different pore-surface functionalities, such as Lewis acidity/basicity and hydrophobicity and -philicity, etc., have been explored,[6] modification of the pore surface for specific applications is still a difficult challenge. Two general strategies to generate functionalized pore surfaces have been proposed:[1a] (a) the incorporation of coordinatively unsaturated metal centers (UMCs) and (b) the introduction of guest-accessible organic functional groups. It has been proved that both strategies can improve the host−guest interactions or provide catalytic active sites. In particular, the latter strategy can not only change the properties of the pore surface but also open the possibility of further modification of the surface by the so-called "postsynthetic" approach,[7] which takes advantage of the reactivity of the functional groups on the pore surface.

The carbonyl group possesses high chemical reactivity and may act as the basic site in base-catalyzed reactions.[8] The incorporation of this group onto the pore surface would constitute a new interaction site for selective sorption and/or catalysis inside the pores. For this purpose, we design a new dicarboxylate ligand bearing a carbonyl group, fluorenone-2,7-dicarboxylic acid (H_2FODC; Scheme S1 in the Supporting Information, SI). Herein, we report the synthesis, structure, and absorption properties of a novel 3D porous Zn^{II} MOF with this ligand. The material is unique in the following aspects: (i) It contains a unique layer based on unprecedented hexa- and trinuclear motifs with glycolate dianions ($[OCH_2CH_2O]^{2-}$) as multiconnecting bridges, and the layers are pillared by $FODC^{2-}$ ligands. (ii) The resulting framework

*To whom correspondence should be addressed. E-mail: eqgao@chem.ecnu.edu.cn.

(1) (a) Hasegawa, S.; Horike, S.; Matsuda, R.; Furukawa, S.; Mochizuki, K.; Kinoshita, Y.; Kitagawa, S. *J. Am. Chem. Soc.* **2007**, *129*, 2607–2614. (b) Dybtsev, D. N.; Nuzhdin, A. L.; Chun, H.; Bryliakov, K. P.; Talsi, E. P.; Fedin, V. P.; Kim, K. *Angew. Chem., Int. Ed.* **2006**, *45*, 916–920.

(2) (a) Koh, K.; Wong-Foy, A. G.; Matzger, A. J. *Angew. Chem., Int. Ed.* **2008**, *47*, 677–920. (b) Wang, X.-S.; Ma, S.; Sun, D.; Parkin, S.; Zhou, H.-C. *J. Am. Chem. Soc.* **2006**, *128*, 16474–16475. (c) Pan, L.; Olson, D. H.; Ciemnolonski, L. R.; Heddy, R.; Li, J. *Angew. Chem., Int. Ed.* **2006**, *45*, 616–619.

(3) (a) Düren, T.; Bae, Y.-S.; Snurr, R. Q. *Chem. Soc. Rev.* **2009**, *38*, 1237–1247. (b) Ma, L.; Abney, C.; Lin, W. *Chem. Soc. Rev.* **2009**, *38*, 1248–1256. (c) Czaja, A. U.; Trukhan, N.; Müller, U. *Chem. Soc. Rev.* **2009**, *38*, 1284–1293. (d) Murray, L. J.; Dincă, M.; Long, J. R. *Chem. Soc. Rev.* **2009**, *38*, 1294–1314. (e) Lee, J. Y.; Farha, O. K.; Roberts, J.; Scheidt, K. A.; Nguyen, S. T.; Hupp, J. T. *Chem. Soc. Rev.* **2009**, *38*, 1450–1459. (f) Li, J.-R.; Kuppler, R. J.; Zhou, H.-C. *Chem. Soc. Rev.* **2009**, *38*, 1477–1504.

(4) (a) Eddaoudi, M.; Moler, D. B.; Li, H.; Chen, B.; Reineke, T. M.; Keeffe, M. O.; Yaghi, O. M. *Acc. Chem. Res.* **2001**, *34*, 319–330. (b) Ockwig, N. W.; Delgado-Friedrichs, O.; O'Keeffe, M.; Yaghi, O. M. *Acc. Chem. Res.* **2005**, *38*, 176–182. (c) Tranchemontagne, D. J.; Mendoza-Cortés, J. L.; O'Keeffe, M.; Yaghi, O. M. *Chem. Soc. Rev.* **2009**, *38*, 1257–1283.

(5) (a) Bai, Y. L.; Tao, J.; Huang, R. B.; Zheng, L. S. *Angew. Chem., Int. Ed.* **2008**, *120*, 5424–5427. (b) Wang, X.-L.; Qin, C.; Lan, Y.-Q.; Shao, K.-Z.; Su, Z.-M.; Wang, E.-B. *Chem. Commun.* **2009**, 410–412. (c) Perry, J.; Perman, J. A.; Zaworotko, M. J. *Chem. Soc. Rev.* **2009**, *38*, 1400–1417.

(6) (a) Wu, C.-D.; Hu, A.; Zhang, L.; Lin, W. *J. Am. Chem. Soc.* **2005**, *127*, 8940–8941. (b) Fujita, M.; Kwon, Y. J.; Washizu, S.; Ogura, K. *J. Am. Chem. Soc.* **1994**, *116*, 1151–1152. (c) Choi, H. J.; Suh, M. P. *J. Am. Chem. Soc.* **2004**, *126*, 15844–15851. (d) Seo, J. S.; Whang, D.; Lee, H.; Jun, S. I.; Jeon, Y. J.; Kim, K. *Nature* **2000**, *404*, 982–986. (e) Pan, L.; Liu, H.; Lei, X.; Huang, X.; Olson, D. V.; Turro, N. J.; Li, J. *Angew. Chem., Int. Ed.* **2003**, *115*, 560–564.

(7) (a) Gadzikwa, T.; Farha, O. K.; Mulfort, K. L.; Hupp, J. T.; Nguyen, S. T. *Chem. Commun.* **2009**, 3720–3722. (b) Burrows, D.; Frost, C. G.; Mahon, M. F.; Richardson, C. *Angew. Chem., Int. Ed.* **2008**, *47*, 8482–8486. (c) Wang, Z.; Cohen, S. M. *Chem. Soc. Rev.* **2009**, *38*, 1315–1329 and references cited therein.

(8) Uemura, T.; Kitaura, R.; Ohta, Y.; Nagaoka, M.; Kitagawa, S. *Angew. Chem., Int. Ed.* **2006**, *45*, 4112–4116.

Published on Web 09/10/2010

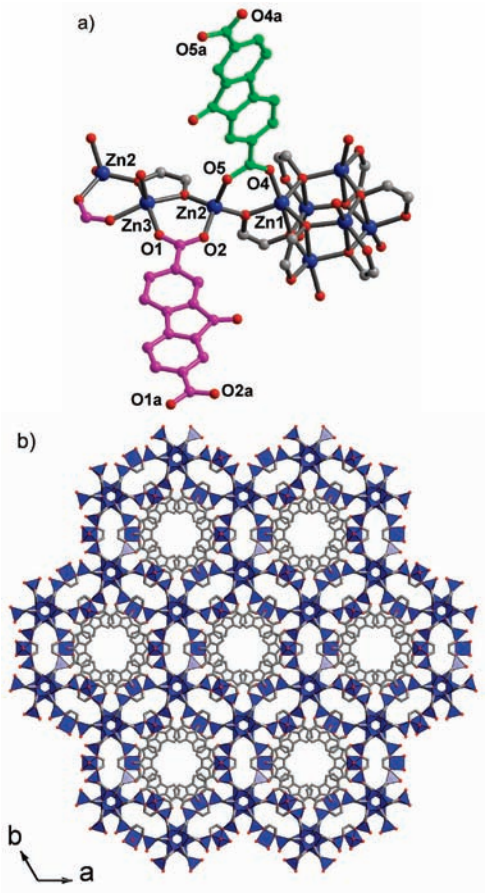

Figure 1. (a) View showing the coordinated environments, the hexagonal prismatic cluster, the trinuclear planar cluster, and the intralayer (purple) and interlayer (green) FODC linkers. (b) Layer structure viewed down the *c* axis. Color code: Zn, blue; O, red; C, gray.

contains a 3D interconnected pore system with large chambers and small channels, and the pore surface is decorated by both carbonyl functionalities and potential UMCs.

The solvothermal reaction of H_2FODC with $Zn(OAC)_2 \cdot 2H_2O$ in a mixture of *N*,*N*′-dimethylacetamide (DMA) and glycol afforded orange hexagonal prismatic crystals of $[Zn_5(FODC)_2(OCH_2CH_2O)_3(H_2O)] \cdot 4DMA \cdot 5.5H_2O$ (**1**). According to single-crystal X-ray crystallography, compound **1** crystallizes in the high-symmetry hexagonal $P6_3/mcm$ space group with three Zn^{2+} ions, two glycolate dianions, two $FODC^{2-}$ ligands, and one coordinated H_2O molecule in the asymmetric unit. The 3D structure consists of zinc−glycolate−FODC layers pillared by $FODC^{2-}$ ligands. The glycolate dianions display two unusual bridging modes: the $\mu_{4.32}$ mode bridging four Zn^{2+} ions through μ_3- and μ_2-O atoms and the $\mu_{3.22}$ mode bridging three Zn^{2+} ions through two μ_2-O atoms.[9] Zn1 adopts the trigonal-bipyramidal geometry completed by three μ_3-O atoms and a μ_2-O atom from three $\mu_{4.32}$-glycolate dianions and a carboxylate O atom from $FODC^{2-}$ ligands (Figure 1a). Six Zn1 atoms are linked together by six μ_3-O groups to form a hexagonal prismatic core of $[Zn_6(\mu_3\text{-}O)_6]$, for which the hexagonal basal plane is defined by alternating Zn1 and μ_3-O atoms and the lateral edge by Zn1−μ_3-O bonds (Figure 1a). The $\{Zn_6O_6\}$ core is unprecedented in the domain of MOFs and has only been observed in a zinc phosphazenate molecule,[10] where the zinc oxide core is sandwiched between (or stablilized by) two bowl-shaped $(Et_2Zn)_3(RNH)_6P_3N_3$ templating segments. Differently, the $\{Zn_6O_6\}$ core in **1** is surrounded and stabilized by six glycolate ligands, which span over the lateral edges of the prism in the alternating up-and-down mode, resulting in an unprecedented $[Zn_6(OCH_2CH_2O)_6]$ cluster. Also, unprecedentedly, three Zn atoms (two Zn2 and a Zn3) are linked by glycolate dianions and carboxylates to generate a trinuclear cluster in which the central Zn3 is chelated by $\mu_{3.22}$-OCH_2CH_2O and connected to Zn2 through μ_2-O and μ_2-COO. The Zn3 site has the square-pyramidal environment furnished by glycolate and carboxylate O atoms in the basal plane and a water ligand at the apex and thus defines a potential UMC upon removal of the coordinated water molecule. The trinuclear $[Zn_3(\mu_{3.22}\text{-}OCH_2CH_2O)(\mu_2\text{-}COO)_2]$ motif is quasi-plannar and serves as a bridging moiety between the hexanuclear clusters. As shown in Figure 1a, Zn2 is tetrahedrally coordinated and connected to Zn1 through μ_2-O from $\mu_{4.32}$ glycolate and a carboxylate bridge in the syn−syn mode, and hence the hexanuclear prismatic clusters and the trinuclear motifs are linked into an extended 2D honeycomb network of $[Zn_5(OCH_2CH_2O)_3(COO)_4]$ along the *ab* plane (Figure S1 in the SI).

There are two independent sets of $FODC^{2-}$ ligands, all being bisected by crystallographic mirror planes and adopting the same coordination mode. One set serves as intralayer bridges, with each ligand bridging two Zn2−Zn3 pairs from different trinuclear motifs in the same layer. The intralayer bridges reinforce the 2D layer and reduce the dimensions of the hexagonal windows of the layer (Figure 1b). The window is lined with C−H groups, and the shortest distance from H to the window axis is 3.35 Å. The other set of $FODC^{2-}$ ligands serves as interlayer linkers, with each bridging two Zn1−Zn2 pairs from different layers. This generates a 3D pillar-layered MOF in which the neighboring hexagonal prismatic motifs from different layers are linked via three equivalent $FODC^{2-}$ ligands related by C_3 rotation (Figure 2a). As shown in Figure 2b, the interlayer space contains "islands" of ligand triplets, and the interlayer voids may be viewed as interconnected trigonal-prismatic chambers. The dimensions of the chamber are about 20 Å (the basal edge of the prism) × 12 Å (the height of the prism), and the interconnecting apertures are about 4 Å wide (the van der Waals radii of the relevant atoms have been subtracted in the dimensions). Thus, taking into account the windows of the layers, the pore in **1** is a 3D interconnected system that contains large chambers and small interconnecting channels. *PLATON* calculations[11] suggest that the free pore volume is 10790.0 and 11096.4 $Å^3$ per unit cell (51.2% and 52.7% of the crystal volume) for the framework with and without coordinated water molecules, respectively. The large "void" space is occupied by DMA and water guest molecules in the as-synthesized materials.

It is interesting to note that the pore surface is furnished with carbonyl groups arising from the interlayer ligands and pointing toward the centers of the large chambers. These functional groups could provide uniform sites for host−guest interactions. Moreover, the water molecules coordinated to the Zn3 sites also

(9) We have used the Harris notation for the coordination modes. See: Coxall, R. A.; Harris, S. G.; Henderson, D. K.; Parsons, S.; Tasker, P. A.; Winpenny, R. E. P. *J. Chem. Soc., Dalton Trans.* **2000**, 2349–2356. See also Scheme S2 in the SI.

(10) Boomishankar, R.; Richards, P. I.; Steiner, A. *Angew. Chem., Int. Ed.* **2006**, *45*, 4632–4634.

(11) Spek, L. *J. Appl. Crystallogr.* **2003**, *36*, 7–13.

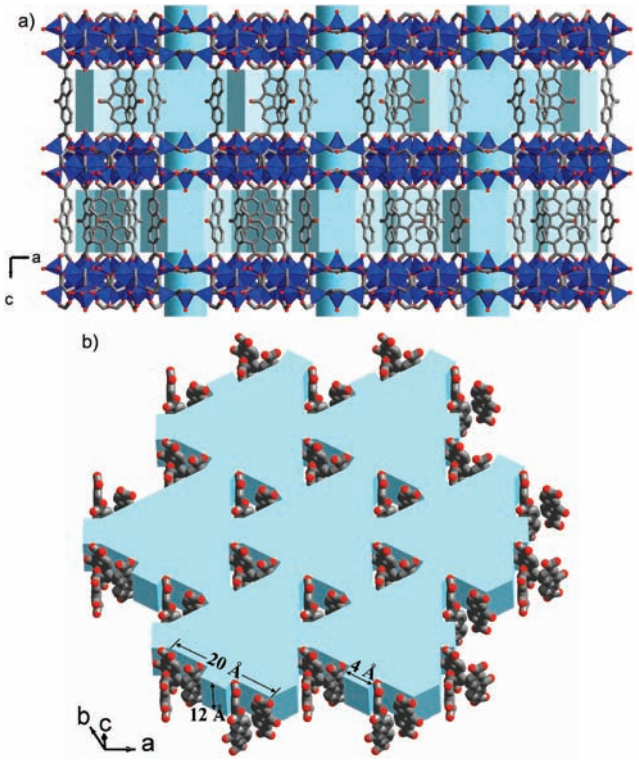

Figure 2. (a) 3D pillar-layered framework. The cyan area highlights the void space. (b) View of the interlayer space with "islands" of ligand triplets.

point toward the chamber centers. The release of the water molecules could leave uniformly distributed UMCs in the evacuated pore, providing additional sites for host−guest interactions.

Thermogravimetric analysis (TGA) suggests that **1** loses all of its solvent molecules (including the coordinated water) upon heating to 300 °C. IR spectra suggest that the coordinated water molecules are at least partially retained upon heating at 150 °C under vacuum and can be completely removed upon further heating to 220 °C. Powder X-ray diffraction (PXRD) measurements (see the SI) reveal that the porous framework remains essentially unchanged upon desolvation, although the crystallinity is somewhat reduced. The permanent porosity is confirmed by N_2 and H_2 gas sorption at 77 K. The PXRD patterns of the activated samples before and after sorption show no appreciable difference (see the SI), suggesting the intactness of the structure. The partially desolvated material (**1a**) activated at 150 °C exhibits rapid N_2 sorption below $P/P_0 = 0.1$, and then the uptake increases gradually until $P/P_0 = 1$ (Figure 3). The Langmuir surface area is 1408 m^2/g, with the total pore volume being 0.538 cm^3/g. When the sample is activated at 220 °C to give the fully desolvated material (**1b**), the Langmuir surface area value is increased to 1603 m^2/g, with a total pore volume of 0.603 cm^3/g. The increases in the initial adsorption, surface area, and adsorption capacity upon full desolvation may be attributable to the removal of the coordinated water molecules and the creation of the UMCs.[12]

Obvious hysteresis behaviors at $P/P_0 > 0.45$ are present in the N_2 adsorption−desorption isotherms of both **1a** and **1b**, indicating the mesoporosity of the samples. The pore-size distribution calculations (Figure S5 in the SI) using the desorption data

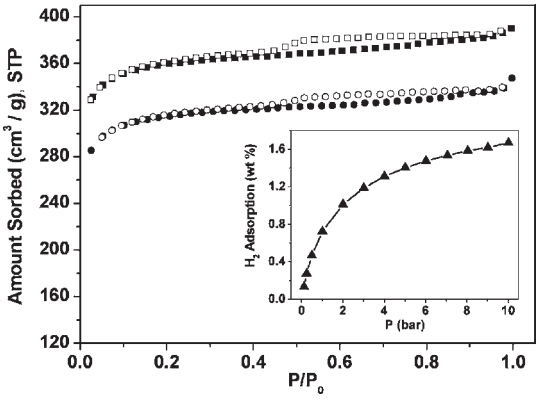

Figure 3. N_2 adsorption isotherms of the partially (circle) and completely (square) desolvated materials at 77 K. Adsorption and desorption data are shown as filled and open symbols, respectively. H_2 (inset) adsorption isotherm measured at 77 K for **1b**.

suggested a distribution of mesopores around 3.9 nm for both materials. Similar mesoporosities have been observed in some other MOFs that are crystallographically microporous and were thought to originate most probably from intercrystalline void spaces in the samples.[13] It has been proposed that the mesopores are related to the coalescence of pores and the formation of fractal networks.[13a] Finally, a gravimetric H_2 sorption isotherm of the fully desolvated material **1b** was recorded from 0 to 10 bar at 77 K, as shown in Figure 3 (inset). The material displays a hydrogen uptake of 1.67 wt % at 77 K and 10 bar.

In summary, we have successfully prepared a novel 3D pillar-layered porous MOF from a carbonyl-functionalized dicarboxylate ligand. The MOF consists of unique zinc−glycolate−carboxylate layers in which rare hexanuclear $[Zn_6(OCH_2CH_2O)_6]$ clusters with hexagonal-prismatic $[Zn_6(\mu_3\text{-}O)_6]$ cores are connected by trinuclear-planar $[Zn_3(OCH_2CH_2O)(COO)_2]$ clusters. The 3D pore system in the materials contains large interlayer chambers and small interconnecting channels. The recognition of the polynuclear clusters held by the bridging glycolate dianion may offer a new approach for the construction of MOFs with new structures and properties. Moreover, it is interesting to note that the material is furnished simultaneously with the carbonyl group (Lewis basic site) and the UMCs (Lewis acid site) on the pore surface. Although this preliminary investigation indicates that the present material is not stable enough to resist common solvents, studies along this line may create new bifunctional materials promising for heterogeneous catalysis.[14]

Acknowledgment. This work was supported by the NSFC (Grant 20771038) and Shanghai Leading Academic Discipline Project (Project B409).

Supporting Information Available: Experimental procedure, crystallographic details, X-ray crystallographic data in CIF format, supplementary figures, TGA data, vacuum IR spectra, and PXRD patterns. This material is available free of charge via the Internet at http://pubs.acs.org.

(12) Chen, N.; Ockwig, W.; Millward, A. R.; Contreras, D. S.; Yaghi, O. M. *Angew. Chem., Int. Ed.* **2005**, *44*, 4745–4749.

(13) (a) Tsao, C.-S.; Yu, M.-S.; Chung, T.-Y.; Wu, H.-C.; Wang, C.-Y.; Chang, K.-S.; Chen, H.-L. *J. Am. Chem. Soc.* **2007**, *129*, 15997–16004. (b) Lee, J.-Y.; Li, J.; Jagiello, J. *J. Solid State Chem.* **2005**, *178*, 2527–2532. (c) Vishnyakov, A.; Ravikovitch, P. I.; Neimark, A. V.; Bulow, M.; Wang, Q. M. *Nano Lett.* **2003**, *3*, 713–718. (d) Saha, D.; Deng, S.; Yang, Z. *J. Porous Mater.* **2009**, *16*, 141–149.

(14) (a) Kadib, A. E.; Molvinger, K.; Bousmina, M.; Brunel, D. *Org. Lett.* **2010**, *12*, 948–951. (b) Katayama, S.; Nonaka, Y.; Iwata, K.; Kubo, Y.; Yamada, N. *Adv. Mater.* **2005**, *17*, 2596–2599.